

Magnetic screening in proximity-coupled superconductor/normal-metal bilayers

Michael S. Pambianchi, Jian Mao, and Steven M. Anlage

Center for Superconductivity Research, Physics Department, University of Maryland, College Park, Maryland 20742-4111

(Received 22 July 1994)

The electrodynamics of a metallic surface layer in proximity contact to a superconductor are considered. The surface region is modeled as an idealized proximity-coupled superconductor/normal-metal (S/N) bilayer. Analytical expressions for the magnetic-field penetration into the sample are obtained. The behavior of the model and its applicability to magnetic-screening-length measurements on artificial and naturally occurring S/N bilayer superconductors are discussed in various limits. Calculations of the effective penetration depth $\lambda_{\text{eff}}(T)$ reveal that unconventional penetration depth temperature dependences, such as $\Delta\lambda_{\text{eff}}(T) \sim T$ found in $\text{YBa}_2\text{Cu}_3\text{O}_{7-\delta}$ crystals, are qualitatively reproduced with this model.

I. INTRODUCTION

Measurements of the surface impedance of superconductors are very sensitive to the properties of the region near the surface of the sample. However, superconducting samples can have a region of nonsuperconducting material on the surface. This may be due to oxidation in the case of conventional superconductors, or to oxygen loss in the case of cuprate superconductors. Since surfaces can support large gradients in chemical composition, the electrodynamic properties of the material can vary on length scales comparable to the magnetic screening length of the bulk superconductor (typically $\sim 10^2\text{--}10^3$ Å).

Two examples of superconductors with surfaces not characteristic of the bulk are Nb and $\text{YBa}_2\text{Cu}_3\text{O}_7$ (YBCO). Niobium can develop metallic surface suboxides, NbO_x , $x \leq 1$, which have superconducting transition temperatures T_c below that of bulk Nb.¹ These suboxides penetrate the bulk from the surface in a rather complicated way, and can influence surface impedance measurements.^{1,2} The cuprate superconductor YBCO is known to have oxygen deficiencies near the surface,³ with T_c decreasing monotonically with increasing oxygen deficiency. Experiments on YBCO thin films have shown a wide array of electrodynamic properties, depending sensitively on the history of film oxidation.⁴

Superconducting cavity perturbation measurements⁵⁻⁷ on these two materials show different results for the magnetic-screening-length temperature dependence $\Delta\lambda(T) = \lambda(T) - \lambda(T_0)$, where T_0 is some fixed low temperature. While pure Nb shows $\Delta\lambda(T) \sim T^{-1/2} \exp(-\Delta/k_B T)$ for $T < T_c/2$, consistent with s -wave superconductivity, YBCO crystals exhibit a distinct linear dependence $\Delta\lambda(T) \sim T$ at low temperatures,^{6,7} consistent with nodes in the energy gap. This linear temperature dependence of $\Delta\lambda(T)$ is very reminiscent of surface impedance measurements on intentionally prepared proximity-coupled Nb/Al bilayers, which also show a clear linear-in- T dependence for the effective screening length at low temperatures.⁸ It is also qualitatively similar to $\Delta\lambda(T)$ measurements on Ag/Pb samples

in superconductor-insulator-normal-metal-superconductor (SINS') tunnel junctions⁹ and mutual inductance measurements on NbN/Al bilayer films,¹⁰ both of which were clear manifestations of the proximity effect in normal-metal surface layers. A strong temperature dependence of $\Delta\lambda(T)$ at low temperature, although not linear, was predicted by Kresin¹¹ for proximity-coupled S/N bilayers. The striking similarity between $\Delta\lambda(T)$ data on YBCO crystals and these samples suggests that the proximity effect might produce such behavior in a YBCO sample with a degraded surface. In this paper we demonstrate that metallic surface layers in proximity contact with nominally pure superconductors alter the electrodynamics of the surface and produce effects which mask the intrinsic behavior of superconductors in surface impedance measurements.

II. MODEL

We introduce a model¹² which idealizes the degraded surface of a superconducting material. The model addresses the screening of magnetic field in a proximity-coupled superconductor/normal-metal (S/N) bilayer, and has been applied successfully to understanding screening in artificially produced S/N bilayers.⁸ It consists of a superconductor S which extends from $x=0$ to d_S and a normal film N which extends from $x=0$ to $x=-d_N$ (see inset of Fig. 1). The S/N interface at $x=0$ is assumed to be sharp and clean enough so that proximity coupling takes place between the two metals. The bilayer as a whole has a superconducting transition temperature T_{cNS} , and the normal metal itself is permitted to have a lower bulk superconducting transition temperature T_{cN} , which may be set to zero. We assume that both metals are in the dirty limit. For temperatures $T > T_{cN}$, the normal metal has a coherence length $K^{-1}(T)$ given by the solution to¹³ $\ln(T/T_{cN}) = \psi(1/2) - \psi[1/2 - \hbar D_N K^2 / (4\pi k_B T)]$, where ψ is the digamma function, $D_N = v_{FN} l_{\text{mfp}} / 3$, and v_{FN} and l_{mfp} are the Fermi velocity and quasiparticle mean free path in N , respectively. If $T_{cN} = 0$, we use $K^{-1}(T) = (\hbar D_N / 2\pi k_B T)^{1/2}$. Finally, the S and N films are given spatially dependent magnetic penetration depths $\lambda_S(x, T)$ and $\lambda_N(x, T)$, the

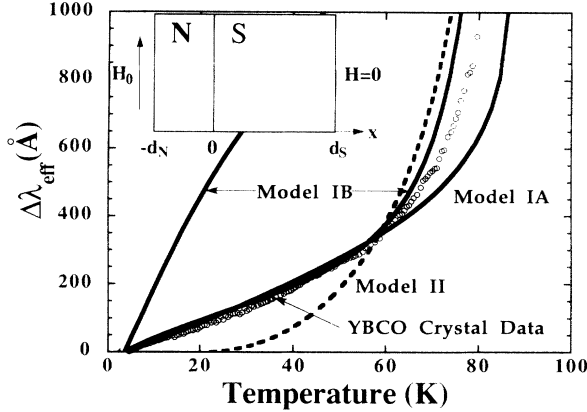


FIG. 1. Representative plots of $\Delta\lambda_{\text{eff}}(T) = \lambda_{\text{eff}}(T) - \lambda_{\text{eff}}(4.2 \text{ K})$ for proximity bilayer model I in the limit $d_N \gg \lambda_N(0,0)$, using $T_{cN} = 10^{-3} \text{ K}$ and $\lambda_S(0) = 1400 \text{ \AA}$. Shown are model I_A [$d_N = 1000 \text{ \AA}$, $K^{-1}(T_{cNS}/2) = 326 \text{ \AA}$, $\lambda_N(0,0) = 20 \text{ \AA}$], model I_B [upper: $d_N = 1000 \text{ \AA}$, $K^{-1}(T_{cNS}/2) = 15 \text{ \AA}$, $\lambda_N(0,0) = 20 \text{ \AA}$], model I_B [lower: $d_N = 300 \text{ \AA}$, $K^{-1}(T_{cNS}/2) = 326 \text{ \AA}$, $\lambda_N(0,0) = 20 \text{ \AA}$]. Also shown is model II [$d_N = 10 \text{ \AA}$, $K^{-1}(T_{cNS}/2) = 326 \text{ \AA}$, $\xi_S = 15 \text{ \AA}$, $D_S = D_N$]. Open circles are $\Delta\lambda_{ab}(T)$ data for a YBa₂Cu₃O₇ single crystal (J. Mao *et al.*, Refs. 6 and 7). Inset: S/N bilayer geometry and magnetic-field boundary conditions.

forms of which are based on a proximity-effect theory developed in the Ginzburg-Landau formalism.^{13,14} Although this theory is only valid in the limit of vanishingly small pair potential, there are many precedents for extending the results to low temperatures.^{9,13,15,16} We identify two distinct models for the local screening length, one due to Deutscher (model I), and the other due to de Gennes (model II).

In model I we assume that the N layer is active in screening due to a nonzero proximity-induced pair potential $\Delta_N(x, T)$,¹⁷ and that the S layer is unaffected by the presence of the N layer, so that $\lambda_S(x, T) = \lambda_S(T)$ is uniform across the S layer. $\lambda_S(T)$ is given the full BCS temperature dependence calculated by Mühlshlegel.¹⁸ In the normal layer we take $\lambda_N(x, T)^{-1} \sim \Delta_N(x, T)$, a widely accepted approximation for the spatial dependence of the screening length.^{13,14,17} Previous measurements^{15,16} of the effective screening length in S/N bilayers were relatively insensitive to λ_N , however, so the exact temperature dependence of λ_N remains unresolved. We therefore separate model I into two versions with different temperature dependences. In model I_A we assume that the only temperature dependence in λ_N comes from Δ_N , an assumption which led to good agreement between theory and experiment in the SINS' tunneling measurements of Simon and Chaikin.⁹ In model I_B, we follow the calculation of Deutscher *et al.*^{13,14} and take

$$\lambda_N(x, T)^{-2} = \mu_0 \sigma_N / (\hbar \pi k_B T) \Delta_N^2(x, T) \times \psi' [1/2 - \hbar D K^2 / (4\pi k_B T)],$$

where σ_N is the normal-state conductivity of the N film. Model I_B essentially adds a factor of $T^{1/2}$ to the tempera-

ture dependence of $\lambda_N(x, T)$ used in model I_A.¹⁹

By contrast, we assume in model II that the N layer does no screening at all [$\lambda_N(x) \rightarrow \infty$, and $d_N \ll \delta_N$, the normal-metal skin depth]. The S layer, however, suffers a suppressed order parameter within a distance ξ_S of the S/N interface, and has a correspondingly enhanced penetration depth:

$$\lambda_S(x, T) = \lambda_{S\text{bulk}}(T) \coth[(x - x_0)/2^{1/2} \xi_S(T)],$$

where x_0 is on the order of $-\xi_S$, the coherence length in S .²⁰ In all models, we ignore normal currents in both the N and S films, since λ_N and λ_S are typically both much less than the normal-metal skin depths in N and S , even at microwave frequencies.

To find the fields and currents in the S/N bilayer in any of these models, Maxwell's equations are solved using a generalized London equation to relate the magnetic field and supercurrent,⁹ $\nabla \times (\lambda^2 \mathbf{J}_s) = -\mathbf{H}$. This yields an equation for the tangential magnetic field as a function of depth in the bilayer:

$$H''(x) + \frac{2}{\lambda(x)} \lambda'(x) H'(x) - \frac{1}{\lambda^2(x)} H(x) = 0, \quad (1)$$

which is solved with boundary conditions $H(-d_N) = H_0$, $H(d_S) = 0$ (see the inset of Fig. 1), $H(0)$ continuous, and²¹

$$\lambda_N(0, T)^2 H'(x)|_{x=0^-} = \lambda_S(0, T)^2 H'(x)|_{x=0^+}.$$

Since we neglect losses, this equation is strictly correct only at dc. We also assume that a supercurrent $\mathbf{J}_s(x)$ flows in the proximity-coupled normal film, and that a local relation exists everywhere between fields and currents.²²

Analytical solutions for $H(x)$ and $\mathbf{J}_s(x)$ can be obtained only for special choices of $\lambda(x)$ in Eq. (1). For model I we have obtained a solution for $H(x)$ and $\mathbf{J}_s(x)$ in both the N and S layer using a simple exponential dependence for the pair potential in N , $\Delta_N(x) = \Delta_N(0) e^{+Kx}$.²³ We then have $\lambda_N(x, T) = \lambda_N(0, T) e^{-Kx}$, yielding the following expression for $H_I(x)$:²⁴

$$\begin{aligned} H_{I,N}(x, T) &= ApI_1(p) + BpK_1(p) \quad (-d_N \leq x \leq 0), \\ H_{I,S}(x, T) &= Ce^{x/\lambda_S(T)} + De^{-x/\lambda_S(T)} \quad (0 \leq x \leq d_S), \end{aligned} \quad (2)$$

where $p = p(x, T) = e^{K(T)x} / [K(T)\lambda_N(0, T)]$ is a dimensionless parameter, and I_1 and K_1 are modified Bessel functions of the first and second kind, respectively. The constants A, B, C, D are found by enforcing the boundary conditions mentioned above. This expression for $H_I(x)$ applies for both models I_A and I_B.

For model II an analytical solution was found by de Gennes and Matricon.²⁵ They developed a solution for the vector potential in S , from which the magnetic fields and supercurrents can be found (see the Appendix). This model is simpler because it neglects the N layer electrodynamics, reducing the number of boundary conditions from four to two.

To compare these calculations to experiment, we calculate the inductance of the bilayer. One can write the total energy stored in a superconductor, in both magnetic

fields and supercurrents, as being due to a total inductance: $U_{\text{total}} = \frac{1}{2} L_{\text{total}} I^2$. The total inductance is given by

$$L_{\text{total}} = \frac{\mu_0}{H_0^2} \int_{-d_N}^{+d_S} H^2(x) dx + \frac{\mu_0}{H_0^2} \int_{-d_N}^{+d_S} \lambda^2(x) J_s^2(x) dx, \quad (3)$$

where H_0 is the applied field. The first term is the magnetic inductance for fields stored in the bilayer, while the second term is the kinetic inductance from energy stored in supercurrents flowing in the bilayer. This expression reduces to the total inductance of a superconductor of thickness d_S [$L_{\text{total}} = \mu_0 \lambda_S \coth(d_S/\lambda_S)$] in the limit $d_N \rightarrow 0$.²⁶ We then define an effective penetration depth λ_{eff} associated with the total inductance $L_{\text{total}} = \mu_0 \lambda_{\text{eff}}$. This effective penetration depth can be directly compared to experimentally determined magnetic screening lengths.²⁷

III. RESULTS

Model I has been found to describe $\Delta\lambda_{\text{eff}}(T)$ data on proximity-coupled Nb/Al bilayer films⁸ very well. These samples, which had “artificial” Al metal surface layers ($d_N \leq 600$ Å), were fabricated to simulate naturally occurring metallic surface layers on superconductors. They exhibited very unconventional $\Delta\lambda_{\text{eff}}(T)$ at low temperatures, in contrast to the conventional behavior in pure Nb samples mentioned above. Hence model I may be generally applicable to other superconducting samples which show unusual $\Delta\lambda_{\text{eff}}(T)$ at low temperatures, including YBCO crystals.^{6,7,28} By contrast, model II, which ignores screening in the surface N layer, does not describe data on Nb/Al bilayers well. In particular, it predicts little departure from pure Nb behavior at low temperature. It therefore is clear that screening in the proximity-coupled surface N layer cannot be neglected.

To better understand the range of extrinsic effects caused by metallic surface layers, we consider model I in a few limiting cases.

A. $\lambda_N(0,0) \gg d_N$

Very little screening occurs in the N film in this limit. The results of models I_A and I_B show that the underlying temperature dependence of the screening length in S dominates $\Delta\lambda_{\text{eff}}(T)$. This result is essentially independent of the size of the coherence length in N . Moreover, the effect of a thin N layer on the pair potential in S is also very small, so using model II also does not introduce any significant differences from the case of a bare superconductor. We conclude that thin normal-metal films with very large proximity-induced screening lengths produce virtually no change to the measured penetration depth of the underlying superconductor, in any model.

B. $\lambda_N(0,0) \ll d_N$

If in addition $K^{-1} \gg d_N$, significant screening occurs in the N layer, with the total inductance dominated by magnetic fields and screening currents near the free sur-

face of N . Figure 1 shows several examples of $\Delta\lambda_{\text{eff}}(T)$ in this limit, with $\Delta\lambda_{ab}(T)$ data on a YBCO single crystal^{6,7} shown to set the scale. The results for model II essentially show the BCS s -wave temperature dependence¹⁸ assumed in all cases for the underlying superconductor [with $\lambda_S(0) = 1400$ Å]. However, both models I_A and I_B show $\Delta\lambda(T) \sim T$ over a substantial temperature range for a variety of parameter values. The linear temperature dependence of $\Delta\lambda_{\text{eff}}(T)$ comes primarily from $K^{-1}(T)$ in model I_A , and from $\lambda_N(x, T)$ in model I_B . The normal-metal parameters for two of the plots in Fig. 1 were chosen to match the YBCO crystal data at low temperatures. The value $\lambda_N(0,0) = 20$ Å necessary in both cases to achieve $\Delta\lambda_{\text{eff}}(T) \sim T$ up to 60 K is clearly not appropriate for oxygen-deficient YBCO. Still, the wide range of parameters which give linear behavior, along with our observation of $\Delta\lambda_{\text{eff}}(T) \sim T$ in Nb/Al bilayers,⁸ Simon’s observations in Ag/Pb samples,⁹ and Claassen’s results on NbN/Al bilayers,¹⁰ show that linear temperature dependence of $\Delta\lambda_{\text{eff}}$ results quite generally from a proximity-coupled bilayer model.²⁹

If $K^{-1} \ll d_N$, however, then the local penetration depth at the free surface $\lambda_N(-d_N, T)$ can be very large, allowing the magnetic field to penetrate far into N . Screening currents then flow primarily near the interface between the two metals and the N and S layers both contribute to the total inductance. The upper curve in Fig. 1 has a strong linear-in- T effective penetration depth which comes from contributions of both the S and N layers. Thus a linear-in- T dependence in $\Delta\lambda_{\text{eff}}(T)$ clearly can arise from a proximity layer whenever $\lambda_N(0,0) \ll d_N$.

C. $\lambda_N(0,0) \sim d_N$

In this case a variety of results can be obtained, depending on the parameter values chosen (see Fig. 2). The S and N layers both contribute to the total inductance, giving rise to the somewhat complicated temperature

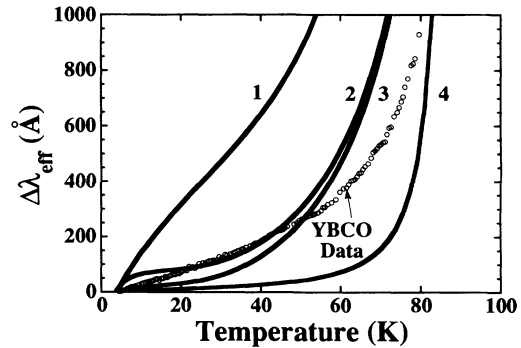


FIG. 2. Representative plots of $\Delta\lambda_{\text{eff}}(T) = \lambda_{\text{eff}}(T) - \lambda_{\text{eff}}(4.2 \text{ K})$ for proximity bilayer model I in the limit $d_N \sim \lambda_N(0,0)$, using $T_{cN} = 10^{-3}$ K and $\lambda_S(0) = 1400$ Å. Shown are model I_A (No. 1) [$d_N = 1000$ Å, $K^{-1}(T_{cNS}/2) = 660$ Å, $\lambda_N(0,0) = 500$ Å], model I_B (No. 2) [$d_N = 500$ Å, $K^{-1}(T_{cNS}/2) = 33$ Å, $\lambda_N(0,0) = 500$ Å], model I_A (No. 3) [$d_N = 1000$ Å, $K^{-1}(T_{cNS}/2) = 326$ Å, $\lambda_N(0,0) = 5000$ Å], and model I_A (No. 4) [$d_N = 10$ Å, $K^{-1}(T_{cNS}/2) = 15$ Å, $\lambda_N(0,0) = 20$ Å]. Open circles are $\Delta\lambda_{ab}(T)$ data for a $\text{YBa}_2\text{Cu}_3\text{O}_7$ single crystal (J. Mao *et al.*, Refs. 6 and 7).

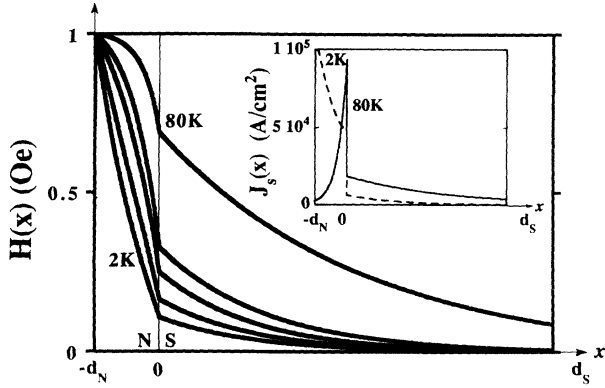


FIG. 3. Magnetic-field penetration profiles at 2, 10, 30, 50, and 80 K for a hypothetical high- T_c superconductor ($d_S = 1 \mu\text{m}$) with a normal-metal surface layer ($d_N = 1000 \text{ \AA}$), using model I_A. Parameter values are $H_{\text{applied}} = 1 \text{ Oe}$, $\lambda_S(0) = 1400 \text{ \AA}$, $\lambda_N(0,0) = 500 \text{ \AA}$, $T_{cNS} = 90 \text{ K}$, $T_{cN} = 10^{-3} \text{ K}$, $K^{-1}(T_{cNS}/2) = 660 \text{ \AA}$. The BCS temperature dependence was used for $\lambda_S(T)$. Inset: Supercurrent density profile at $T = 2 \text{ K}$ (dashed) and $T = 80 \text{ K}$ (solid).

dependences seen in $\Delta\lambda_{\text{eff}}(T)$. A linear-in- T behavior is still generally seen over a limited temperature range, but other behavior, such as quadratic, bilinear, and sublinear temperature dependences are also seen at low temperatures. The variety of results in Fig. 2 is reminiscent of the results on YBCO films by Klein *et al.*, where oxygen annealing times and pressures were varied.⁴ Those results might be qualitatively explained as S/N bilayer samples in which the N film thickness and conductivity were changed by annealing.

The nonlinear temperature dependences in Fig. 2 are associated with a crossover from the case where screening currents flow near the free surface to where screening currents flow near the S/N interface. Figure 3 illustrates this crossover by showing the magnetic field and supercurrent profiles for the sample parameters given in curve 1, Fig. 2. At low temperatures, screening currents flow near the free surface because $K^{-1}(T)$ is large enough for the pair potential $\Delta_N(x)$ to be present throughout N . This causes the magnetic field to decay quickly into N . At high temperatures, however, two things occur. Firstly, $\lambda_N(0, T)$ is large because $\Delta_N(0, T)$ is smaller in magnitude when $T \sim T_{cNS}$. Secondly, $K^{-1}(T)$ is small when

$T \sim T_{cNS}$, so the pair potential decays more quickly into N , increasing $\lambda_N(-d_N, T)$ even more. These two effects together permit magnetic field to penetrate deep into N , and screening currents only flow where appreciable pair potential is present, i.e., just near the S/N interface. This crossover in going from low to high temperatures has been observed experimentally in the strongly sublinear $\Delta\lambda_{\text{eff}}(T)$ seen in Nb/Al (Ref. 8) and Nb/Cu (Ref. 10) bilayers.

IV. SUMMARY

We have presented analytical solutions for two models of magnetic field screening in a proximity-coupled superconductor/normal-metal bilayer, which represents the degraded surface of a superconducting sample. Model II, by neglecting the normal layer electrostatics completely, represents an oversimplification of the problem and cannot reproduce the range of behavior found in samples with artificial metallic surface layers. However, model I, which does assume screening in the normal-metal layer, exhibits a wide range of behaviors, many of which show $\Delta\lambda_{\text{eff}}(T) \sim T$ over some range of temperature. This model, although strictly applicable only near T_{cNS} due to its origin in Ginzburg-Landau theory, successfully reproduced the unusual low-temperature $\Delta\lambda_{\text{eff}}(T)$ data from proximity-coupled Nb/Al bilayers. This suggests that recent experimental results on $\Delta\lambda_{ab}(T)$ in YBCO single crystals and films may be due to proximity-coupled normal layers, though the normal-metal parameters required to reproduce the $\Delta\lambda_{ab}(T) \sim T$ data in YBCO crystals are not consistent with the properties of oxygen-deficient cuprates.

Note added in proof. After completion of this article, it was brought to our attention by J. Halbritter that J. R. Hook has developed a BCS-like model of screening in S/N bilayers similar in spirit to our approach [J. R. Hook, *J. Low Temp. Phys.* **23**, 645 (1976)].

ACKNOWLEDGMENTS

We thank R. W. Simon and M. R. Beasley for seminal discussions about this work, as well as G. Deutscher and C. J. Lobb for further advice and encouragement. We also thank D. H. Wu, A. Das, and S. N. Mao for assistance. This work was supported by NSF Grant No. DMR-9123198.

APPENDIX

Here we give the solution to the generalized London equation [Eq. (1)] for model II, where $\lambda_S(x) = \lambda_{S \text{ bulk}}(T) \coth[(x - x_0)/2^{1/2}\xi_S(T)]$, and there is no screening in the N layer. de Gennes and Matricon earlier found an expression for the vector potential in S for this model.²⁴ The magnetic-field profile is given by $H_{II,N}(x) = H_0$ ($-d_N \leq x \leq 0$) and $H_{II,S}(x) = Cg_1(x) + Dg_2(x)$ ($0 \leq x \leq d_S$), where

$$g_1(x) = \frac{1}{\mu_0} \left\{ -\alpha(s+2a) \cosh^{-(s+2a+1)}(\alpha u) \sinh(\alpha u) {}_2F_1[a, a-c+1, a-b+1; \cosh^{-2}(\alpha u)] \right. \\ \left. - \frac{2\alpha a(a-c+1)}{a-b+1} \cosh^{-(s+2a+3)}(\alpha u) \sinh(\alpha u) {}_2F_1[a+1, a-c+2, a-b+2; \cosh^{-2}(\alpha u)] \right\} \quad (\text{A1})$$

and $g_2(x)$ is identical except that a and b are interchanged. Here, $\alpha = 1/(2^{1/2}\xi_S)$, $s = \{-1 + [1 + 4/(\alpha^2\lambda_{S \text{ bulk}}^2)]^{1/2}\}/2$, $c = -s - 1/2$, $a, b = [-s \pm (s^2 + s)^{1/2}]/2$, $u = x - x_0$, and ${}_2F_1$ is the hypergeometric function. The constants C and D are determined by the boundary conditions on the magnetic field.

- ¹W. Schwarz and J. Halbritter, *J. Appl. Phys.* **48**, 4618 (1977).
- ²J. Halbritter, *Appl. Phys. A* **43**, 1 (1987); *J. Less-Common Met.* **139**, 133 (1988).
- ³E. F. Skelton, A. R. Drews, M. S. Osofsky, S. B. Qadri, J. Z. Hu, T. A. Vanderah, J. L. Peng, and R. L. Greene, *Science* **263**, 1416 (1994).
- ⁴N. Klein, N. Tellmann, H. Schulz, K. Urban, S. A. Wolf, and V. Z. Kresin, *Phys. Rev. Lett.* **71**, 3355 (1993).
- ⁵Steven M. Anlage, Dong-Ho Wu, J. Mao, S. N. Mao, X. X. Xi, T. Venkatesan, J. L. Peng, and R. L. Greene, *Phys. Rev. B* **50**, 523 (1994).
- ⁶Jian Mao, D. H. Wu, S. M. Anlage, S. N. Mao, X. X. Xi, T. Venkatesan, J. L. Peng, and R. L. Greene, *Physica C* (to be published).
- ⁷Jian Mao, D. H. Wu, J. L. Peng, R. L. Greene, and S. M. Anlage (unpublished).
- ⁸M. S. Pambianchi, S. N. Mao, and Steven M. Anlage (unpublished).
- ⁹R. W. Simon and P. M. Chaikin, *Phys. Rev. B* **23**, 4463 (1981); **30**, 3750 (1984).
- ¹⁰J. H. Claassen, J. E. Evetts, R. E. Somekh, and Z. H. Barber, *Phys. Rev. B* **44**, 9605 (1991).
- ¹¹V. Z. Kresin, *Phys. Rev. B* **32**, 145 (1985).
- ¹²M. S. Pambianchi, S. N. Mao, A. Das, and S. M. Anlage, *Bull. Am. Phys. Soc.* **39**, 186 (1994).
- ¹³G. Deutscher and P. G. de Gennes, in *Superconductivity*, edited by R. D. Parks (Dekker, New York, 1969), p. 1005. Note that the coherence length temperature dependence is well approximated by $K^{-1}(T) = K^{-1}(T_{cNS}/2)[(T_{cNS}/2)/T]^{1/2}$, for $T \gg T_{cN}$.
- ¹⁴G. Deutscher, J. P. Hurault, and P. A. van Dalen, *J. Phys. Chem. Solids* **30**, 509 (1969).
- ¹⁵P. G. de Gennes *et al.*, *Quantum Fluids: Proceedings of the Sussex University Symposium*, edited by D. F. Brewer (North-Holland, Amsterdam, 1966), p. 26.
- ¹⁶A. C. Mota, in *Josephson Effect-Achievements and Trends*, edited by A. Barone (World Scientific, Singapore, 1986), p. 248.
- ¹⁷Here, Δ_N is the induced pair potential in the normal metal, $\Delta_N(x, T) = (1/\alpha)[\Delta_N(x)/\Delta_N(0)][\Delta_S(T)/\Delta_S(0)]$, where Δ_S is the bulk gap in the superconductor and $\alpha = V_S/V_N$ is the ratio of the BCS coupling constants in the *S* and *N* layers. See also Ref. 13.
- ¹⁸B. Mühlischlegel, *Z. Phys.* **155**, 313 (1959).
- ¹⁹This expression for $\lambda_N(x, T)$ eventually breaks down because $\lambda_N(x, T \rightarrow 0) = 0$. Also, to good approximation, one can take $\lambda_{N,IB}(x, T) \propto \lambda_{N,IA}(x, T)T^{1/2}$ (for $T \gg T_{cN}$) and we have done so for the calculations shown in Figs. 1 and 2.
- ²⁰P. G. de Gennes, *Superconductivity of Metals and Alloys* (Addison-Wesley, Redwood City, 1989), p. 233.
- ²¹F. London, *Superfluids* (Dover, New York, 1961), Vol. I, p. 34.
- ²²This assumption breaks down when $K^{-1}(T) \gg \lambda_N(x, T)$ and nonlocal electrodynamics must be used. We assume in such cases that $\lambda_N(x, T)$ represents an "effective" local penetration depth which includes the nonlocal effects.
- ²³This choice of $\Delta_N(x)$ violates the boundary condition $d\Delta/dx = 0$ at a free surface. [See, P. G. de Gennes, *Rev. Mod. Phys.* **36**, 225 (1964).] The more correct expression in the "one frequency" approximation is $\Delta_N(x) = \Delta_N(0)\cosh[K(d_N + x)]/\cosh[Kd_N]$, but this yields an intractable equation for $H(x)$ (see Ref. 9). Our approximation yields results nearly identical to those obtained numerically with this expression, but underestimates the screening in the *N* layer near the free surface. This is most noticeable for $Kd_N \sim 1$, but is never significant for the conclusions drawn in this paper.
- ²⁴To solve Eq. (1) with the simplified $\Delta_N(x)$ in model I, we used a change of variable to $p = e^{Kx}/[K\lambda_N(0, T)]$ followed by a transformation to $M(p)$, defined as $H(p) = pM(p)$. This results in the modified Bessel equation of order 1 for $M(p)$ with solutions for $H(x)$ given by the first part of Eq. (2).
- ²⁵P. G. de Gennes and J. Matricon, *Solid State Commun.* **3**, 151 (1965).
- ²⁶The magnetic-field boundary conditions used here are appropriate for the parallel-plate resonator measurements carried out in Refs. 8 and 12. However, if we choose $d_S \gg \lambda_S$, these calculations of λ_{eff} are also appropriate for the cavity perturbation experiments on thick crystals carried out in Refs. 5–7.
- ²⁷Our definition of λ_{eff} differs from the traditional one given by $\lambda_{\text{trad}} = (1/H_0) \int_0^\infty H(x) dx$. These two penetration depths coincide in value when the magnetic field decays exponentially (pure superconductor), but differ in value when there is nonexponential decay of field. Also, the theory of Kresin (Ref. 11) calculates λ_{trad} directly, hence it could not be used for our models of a local screening length.
- ²⁸W. N. Hardy, D. A. Bonn, D. C. Morgan, Ruixing Liang, and Kuan Zhang, *Phys. Rev. Lett.* **70**, 3999 (1993).
- ²⁹The model predictions of $\Delta\lambda_{\text{eff}}(T)$ in Fig. 1 are not quite as linear as the YBCO crystal $\Delta\lambda_{ab}(T)$ data; they always show some curvature, as is also seen in Nb/Al bilayer data. A similar observations can be made about the intrinsic proximity-effect model of the cuprates proposed by Klemm and Liu [R. A. Klemm and S. H. Liu (unpublished)].